

Production of highly charged rare-gas recoil ions by 1.4-MeV/amu U^{44+}

A. S. Schlachter,* W. Groh, and A. Müller

Institut für Kernphysik, Strahlencentrum, Universität Giessen, 6300 Giessen, West Germany

H. F. Beyer and R. Mann†

Gesellschaft für Schwerionenforschung, 6100 Darmstadt, West Germany

R. E. Olson

Department of Physics, University of Missouri-Rolla, Rolla, Missouri 65401

(Received 2 March 1982)

Recoil-ion-production cross sections in rare gases are measured for 1.4-MeV/amu U^{44+} ions and are calculated for 1–5-MeV/amu projectiles in charge state $44+$ with the use of the classical-trajectory Monte Carlo method and the independent-electron model. The calculations reasonably predict the net-charge-production cross sections, which exceed 10^{-13} cm^2 for the heavy rare gases; the calculations are found to underestimate the cross sections for low-charge-state recoil ions and to overestimate the cross sections for high-charge-state recoil ions. The experimental cross sections for production of highly charged recoil ions are found to be large, e.g., greater than 1×10^{-16} cm^2 for production of Ne^{8+} , Ar^{10+} , Kr^{12+} , and Xe^{18+} .

I. INTRODUCTION

Ionization of rare-gas targets by collisions of fast highly charged projectiles was first measured by Cocke,¹ who used a time-of-flight spectrometer to measure recoil-ion-production cross sections for rare gases bombarded by fast chlorine ions in charge states as high as $13+$. Olson² used the classical-trajectory Monte Carlo method and the independent-electron model to calculate recoil-ion-production cross sections for 1-MeV/amu projectiles in charge states $2+$ to $20+$ in He, Ne, and Ar targets. Cocke found, for the systems studied, that the independent-electron model overestimated recoil-ion-production cross sections σ_j for high-charge states j ; an energy-deposition model¹ was found to account for many features of the data. Hvelplund *et al.*³ measured σ_1 and σ_2 for helium targets bombarded by fast ions in charge states as high as $21+$.

Schlachter *et al.*⁴ used the condenser method to measure net-ionization (net-charge-production) cross sections for fast projectiles in rare-gas targets. Net-ionization cross sections σ_+ are given by

$$\sigma_+ = \sum_j j \sigma_j, \quad (1)$$

where j is the recoil-ion charge state and σ_j is the

recoil-ion-production cross section. They used projectiles in charge states from $4+$ to $54+$. They also used the classical-trajectory Monte Carlo (CTMC) method and the independent-electron model to calculate σ_j in rare gases for projectiles in the energy range 1–5 MeV/amu with charge states $5+$ to $80+$. They found that measurements and calculations of net ionization σ_+ agreed generally to within a factor of 2 for a wide range of projectile energies and charge states. They also found a scaling rule for σ_+ .

We report here measurements of recoil-ion charge-state spectra for rare-gas targets bombarded by 1.4 MeV/amu U^{44+} , calculations of σ_j for 1–5-MeV/amu projectiles in charge state $44+$ in rare-gas targets, and experimental σ_j which we obtain by normalization to the previous⁴ σ_+ measurements.

Measurement of recoil-ion-production cross sections is of interest not only for comparison with theory but also because recoil ions can be used for subsequent collision studies.^{5–7}

II. EXPERIMENTAL METHOD

Our measurements were made using a time-of-flight (TOF) coincidence method and recoil-ion

spectrometer (Fig. 1) which has previously been described⁸ for use with slow projectiles. A 1.4-MeV/amu U^{44+} beam from the UNILAC heavy-ion linear accelerator in Darmstadt intersected at a 90° angle a beam of rare-gas atoms emerging from a narrow tube. Slow recoil ions produced in the collision were extracted by a transverse electric field, accelerated, and were then incident on a channeltron that provided a start pulse to a time-to-amplitude converter (TAC). Although the UNILAC beam is pulsed, its time structure was not suitable for the TOF measurements. We used, instead, the fast ions themselves to provide the stop pulse.⁹ The fast ions were incident on a thin carbon foil located several centimeters downbeam from the collision region. Electrons created by passage of a fast ion through the foil were accelerated into the cone of a channeltron that provided a stop pulse to the TAC. This method was used because unacceptable radiation damage was found when the fast beam was incident directly on a solid-state detector. The flight time of the recoil ions is proportional to the square root of the mass-to-charge ratio. Spectra were accumulated on a multichannel analyzer (MCA) or an on-line computer.

A TOF spectrum for 1.4-MeV/amu U^{44+} in Ne is shown in Fig. 2. The shell effect due to the high binding energy of the K electrons in Ne is evident in the large discontinuity between recoil-ion charge states 8+ and 9+. The spectrum in Fig. 2 also shows a background H^+ peak from residual H_2 and H_2O ; since H_2^+ and $^{20}Ne^{10+}$ have the same flight time, this implies that the peak labeled Ne^{10+} includes an admixture of H_2^+ . A TOF spectrum for 1.4-MeV/amu U^{44+} and Xe is shown in Fig. 3. No shell effect is evident, nor was a shell effect observed in similar spectra (not shown) for Ar and Kr

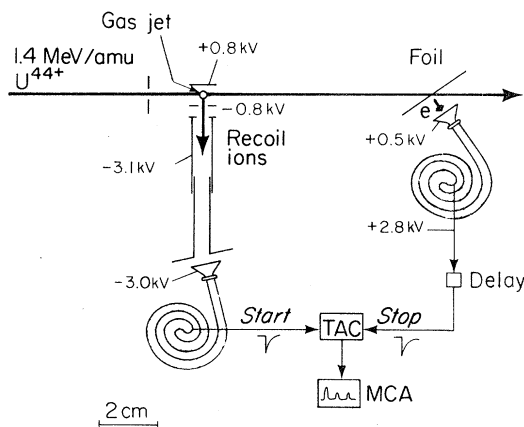


FIG. 1. Schematic diagram of the apparatus.

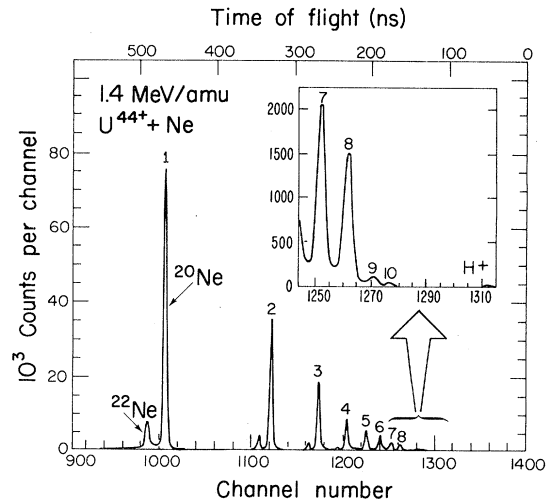


FIG. 2. Recoil-ion charge-state spectrum for 1.4-MeV/amu U^{44+} projectiles in a thin Ne target. Neon recoil charge states 1+ to 10+ are labeled, as is a background H^+ peak. The small peaks to the left of the larger peaks are due to the ^{22}Ne isotope.

targets.

Recoil-ion charge-state fractions were obtained by integration of the TOF peaks. Cross sections were obtained by normalization to the net-ionization cross sections previously obtained by the condenser-plate method.⁴ Relative cross-section uncertainties arising from counting statistics and incomplete peak resolution range from a few percent for large cross sections to about 10% for cross sections of the order of 10^{-16} cm². Absolute cross sec-

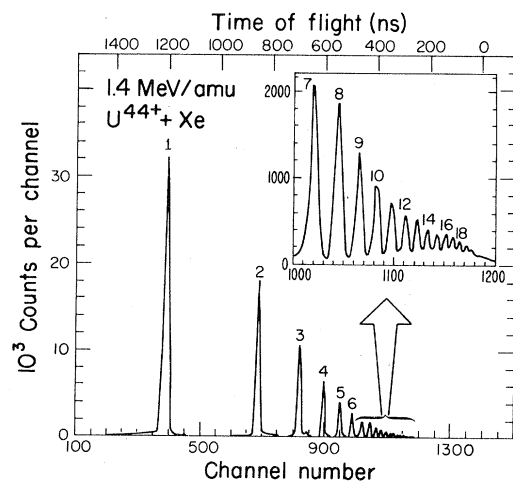


FIG. 3. Recoil-ion charge-state spectrum for 1.4-MeV/amu U^{44+} projectiles in a thin Xe Target. Xenon recoil charge states 1+ to 18+ are labeled.

tions must include an additional 20% uncertainty (30% for Kr and Xe targets) due to uncertainty in the σ_+ values to which cross sections were normalized (σ_+ was estimated for Kr, for which no values are available) and to extrapolation of σ_+ beyond the measured range.

III. THEORETICAL METHOD

The theoretical calculations use the classical-trajectory Monte Carlo method to determine transition probabilities within a one-electron formalism and then extend^{2,4} these transition probabilities to represent a multielectron target by use of the independent-electron model.^{10,11} The independent-electron model requires that the collision be sudden, i.e., so brief that the electrons cannot rearrange themselves during the collision. The model is thus valid only for collision velocities at least several times greater than the orbital velocities of electrons being detached. The model ignores correlation effects between the electrons in a given shell. Also not accounted for are autoionization processes after the collision, which would tend to increase the multiple ionization. Hence, cross sections calculated for production of high states of ionization can only be considered qualitative.

IV. RESULTS AND DISCUSSION

The measured recoil-ion-production cross sections σ_j for 1.4-MeV/amu U^{44+} in rare-gas targets are compared with the calculated values in Fig. 4. Net-ionization cross sections σ_+ are found to be very large and to exceed 10^{-13} cm² for the heavy rare-gas targets. It is clear from the comparison between theory and experiment that σ_+ is reasonably portrayed by the calculations, but that the recoil-ion-production cross sections σ_j predicted by theory are only qualitative.

The deficiencies in the theoretical description probably arise from two approximations that are necessary to perform the calculations. The independent-electron model requires the use of an average binding energy for all electrons within a given shell. If the collision is not sufficiently sudden and the electrons are removed sequentially, this approximation fails,¹ with the result that the last few electrons removed from a shell have a binding energy much larger than the average value of the model. Thus, the calculations will generally overes-

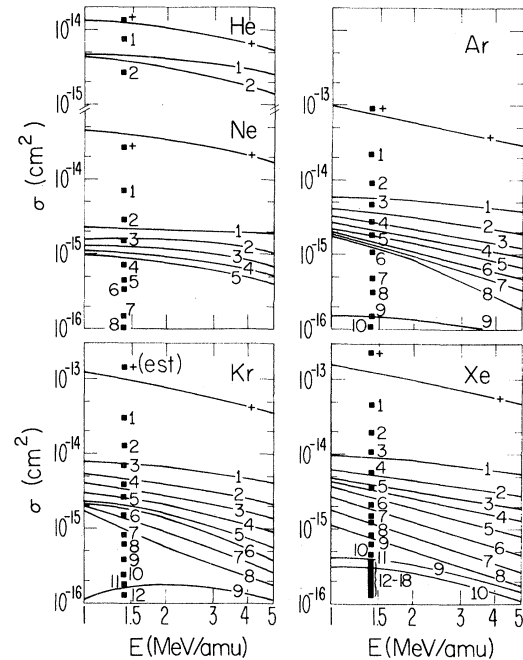


FIG. 4. Cross sections σ_j for production of j -times-ionized recoil ions in He, Ne, Ar, Kr, and Xe targets. The lines are the CTMC calculations for 1–5-MeV/amu projectiles in charge state $44+$, the points are experimental results for 1.4-MeV/amu U^{44+} . The experimental σ_j are normalized to the experimental σ_+ values determined in Ref. 4 (for Kr the σ_+ value shown was estimated).

timate the cross sections for production of the higher charge states.

The theoretical underestimation of the cross sections for low-charge-state recoil-ion production reflects the classical description of the radial electron distribution in the target atom. Tunneling is not allowed classically, hence the electron distribution is not accurately portrayed at large electron-nucleus separations. The low-charge-state recoil ions are generated by large-impact-parameter (soft) collisions that are sensitive to this region of the target's electron distribution. Comparison of theory with experimental data indicates that the collisions are of longer range than we calculate.

Figure 5 shows recoil-ion fractions F_j ($F_j = \sigma_j / \sum \sigma_j$). Theoretical F_j for Ar, Kr, and Xe were found to lie on a single curve; experimental F_j were also found to lie on a common curve (except for F_9 and F_{10} in Ne). The calculations show a pronounced effect due to the shell structure of the target atom, while (except for Ne) the experimental data do not, which indicates that Auger processes must contribute significantly to the production of

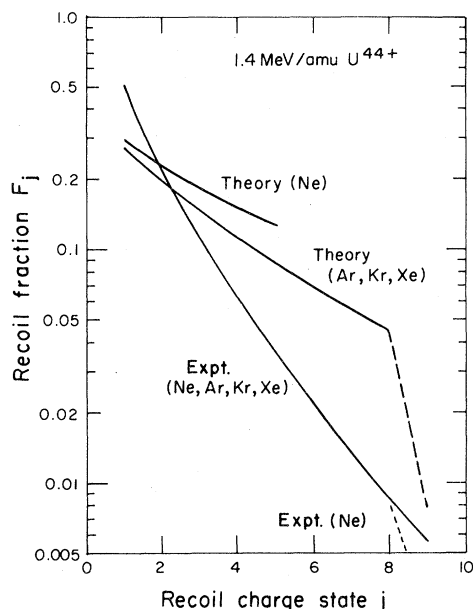


FIG. 5. Recoil-ion charge-state fractions F_j for 1.4-MeV/amu U^{44+} in Ne, Ar, Kr, and Xe. The theoretical lines are the CTMC calculations (Fig. 4). The dashed lines indicate discontinuity due to shell effects.

highly charged recoil ions; this mechanism is not included in the calculations.

Collisions in which rare-gas targets are ionized by fast highly stripped projectiles generally take place at long range. The ionization transition probabilities as a function of impact parameter are calculated using the CTMC method previously discussed. We graphically display in Fig. 6 the long-range nature of these collisions by presenting the sum of the calculated ionization transition probabilities as a function of impact parameter for a 2-MeV/amu fully stripped ion having a charge state 44+ in rare-gas targets. The expectation value for the radius of the outer shell of each rare-gas atom is indicated by an arrow. The collision region is seen to extend to approximately ten times the radii of the outer-electron shells.

The classical-trajectory method was also used to estimate the energy of the recoil ions. This calculation can also be done analytically if one assumes the projectile velocity is much greater than the final velocity of the recoil ion. An illustrative example is the production of Ar^{10+} from U^{44+} impact at 1 MeV/amu. The calculated probabilities for the above ionization transition maximize at an impact parameter $b=2a_0$ and extend to $b=1a_0$ and $3a_0$. The corresponding recoil energies extend from 0.2 to 1.9 eV with a maximum at 0.5 eV; high recoil en-

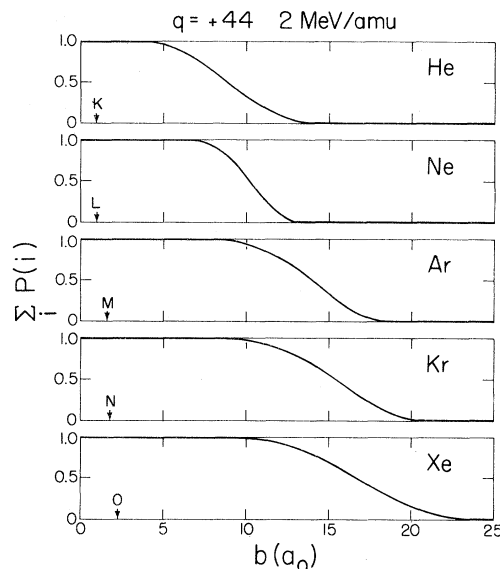


FIG. 6. Total calculated ionization probabilities for a 2-MeV/amu projectile in charge state 44+ in rare-gas targets. The arrows indicate the expectation value for the radius of the outer shell of the target atom.

ergies correspond to small impact parameters.

We have parametrized the theoretical CTMC results and find the recoil energy E_i (in eV) is given by

$$E_i \cong \frac{4 \times 10^{-4} q_p^2 q_i^2}{m_i E_p b^2}, \quad (2)$$

where q_p and q_i are the charge states of the projectile and recoil ions, respectively, m_i is the mass of the target in atomic mass units, E_p is the energy of the projectile in MeV/amu, and b is the impact parameter in units of a_0 . Hence, the recoil-ion energy decreases rapidly with increasing impact parameter and is generally less than 10 eV for the systems studied here.

Equation (2) for the recoil-ion energy, obtained by parametrizing the CTMC calculations, has the same functional dependence as obtained for Rutherford (Coulomb) scattering. However, the coefficient in Eq. (2) is approximately one-half the coefficient for Rutherford scattering.¹² This can be explained by noting that Eq. (2) applies to one-half a collision, since the target is initially neutral. We have assumed that electrons are removed from the target atom at the distance of closest approach, which is approximately equal to the impact parameter. We note that Eq. (2) can be used to determine the impact-parameter dependence of the collision process by measurement of the recoil-ion energy distribution.

In summary, we have presented measured cross sections for rare-gas recoil ions produced by the passage of a fast highly charged ($q=44+$) projectile ion. Experimental and theoretical classical-trajectory Monte Carlo results are compared and the differences discussed. Recoil-ion energies have been calculated and generally range from tenths to a few eV for recoil ions in charge states $q < 10+$ with projectile ions in charge states $q < 50+$ at energies in the low MeV/amu region.

ACKNOWLEDGMENTS

This work was supported in part by the U.S. Department of Energy under contract No. DE-AC02-82ER53128. One of us (A.S.) would like to thank Professor Erhard Salzborn for his hospitality during my stay in Giessen, and to acknowledge support from NATO (Research Grant No. 172.80) and from the Alexander von Humboldt Stiftung.

*Permanent address: Lawrence Berkeley Laboratory, University of California, Berkeley, California 94720.

†Temporary address: J. R. Macdonald Laboratory, Kansas State University, Manhattan, Kansas 66506.

¹C. L. Cocke, Phys. Rev. A **20**, 749 (1979).

²R. E. Olson, J. Phys. B **12**, 1843 (1979).

³P. Hvelplund, H. K. Haugen, and H. Knudsen, Phys. Rev. A **22**, 1930 (1980).

⁴A. S. Schlachter, K. H. Berkner, W. G. Graham, R. V. Pyle, P. J. Schneider, K. R. Stalder, J. W. Stearns, J. A. Tanis, and R. E. Olson, Phys. Rev. A **23**, 2331 (1981).

⁵H. F. Beyer, K. H. Schartner, and F. Folkmann, J. Phys. B **13**, 2459 (1980); R. Mann, F. Folkmann, and H. F. Beyer, *ibid.* **14**, 1161 (1981); R. Mann, H. F. Beyer, and F. Folkmann, Phys. Rev. Lett. **46**, 646 (1981).

⁶C. R. Vane, M. H. Prior, and R. Marrus, Phys. Rev. Lett. **46**, 107 (1981).

⁷C. L. Cocke, R. DuBois, T. J. Gray, E. Justiniano, and C. Can, Phys. Rev. Lett. **46**, 1671 (1981); E. Justiniano, C. L. Cocke, T. J. Gray, R. Dubois, and C. Can, Phys. Rev. A **24**, 2953 (1981).

⁸W. Groh, A. Müller, C. Achenbach, A. S. Schlachter, and E. Salzborn, Phys. Lett. A **85**, 77 (1981).

⁹T. J. Gray, C. L. Cocke, and E. Justiniano, Phys. Rev. A **22**, 849 (1980).

¹⁰J. M. Hansteen and O. P. Mosebekk, Phys. Rev. Lett. **29**, 1361 (1972).

¹¹J. H. McGuire and L. Weaver, Phys. Rev. A **16**, 41 (1977).

¹²W. E. Burcham, *Nuclear Physics/An Introduction*, 2nd ed. (Longman, London, 1973), pp. 93–99.